Ab initio study of the temperature-dependent structural properties of Al(110)

Pawel Scharoch*
Institute of Physics, Wroclaw University of Technology, Wyb.Wyspianskiego 27, 50-370 Wroclaw, Poland
(Received 6 April 2009; revised manuscript received 27 August 2009; published 29 September 2009)

Temperature-dependent structural properties of Al(110) surface have been studied *ab initio* employing the concepts of the potential-energy surface (PES) and the free-energy surface (FES), with the latter based on the harmonic approximation for lattice dynamics. Three effects have been identified as contributing to the temperature-dependent multilayer relaxation: the bulk-substrate thermal expansion, the effect of asymmetry of PESs, and the entropy-driven shift of the minima of FESs. Thanks to the proper choice of constraints for PESs and FESs, it was possible to find relative contribution of the three effects to variation with temperature of the first three interlayer distances. A very satisfactory agreement of the calculation results with experimental data has been obtained. Also, a reference of the theoretical data to the experimentally observed anisotropic surface melting has been noticed. A softening phonon mode has been identified which is responsible for both: the entropy-driven spectacular expansion of the second interlayer distance and the loss of the surface stability. The latter can be associated with the anisotropic surface melting. The methodology applied has been found to be complementary to previous theoretical works [N. Marzari, D. Vanderbilt, A. De Vita, and M. C. Payne, Phys. Rev. Lett. **82**, 3296 (1999); S. Narasimhan, Phys. Rev. B **64**, 125409 (2001)], by offering another point of view and additional insight into the relative contribution of different physical effects to the temperature-dependent structural phenomena in Al(110) surface.

DOI: 10.1103/PhysRevB.80.125429 PACS number(s): 68.35.B−, 68.35.Md, 68.35.Rh

I. INTRODUCTION

Rich phenomenology exhibited by low-Miller-index metal surfaces (100), (110) and (111) has drawn an interest of physicists for a long time. Such phenomena as damped oscillatory multilayer relaxation, surface reconstruction, or premelting have been studied both by experimentalists and theoreticians, using various techniques. Although the basic physical reasons underlying a variety of effects are known (undercoordination of surface atoms, reconfiguration of the free-electron density near the surface, and free-electron density spacial oscillation in the direction vertical to the surface), the physics of particular phenomena is not always fully understood and is still the subject of a dispute. A new, very important, research tool has emerged over the last decades—*ab initio* calculations based on the density-functional theory (DFT). The purely theoretical investigations, with very few approximations, allow for a deep insight into the microscopic properties of a system, and it is only the matter of researcher's invention how to apply the tool and use available data to interpret and understand the experimental observations.

This work deals with a particular case, the Al(110) surface and its temperature-dependent structural properties, although the methodology introduced and some conclusions drawn can be also applied to other metals/surfaces. The system, on the one hand, is relatively simple and on the other, it exhibits an intriguing structural behavior observed in numerous experiments, thus it is a rewarding system to test various theoretical concepts. Two effects have been a subject of interest: the surface multilayer relaxation, in particular, its intriguing temperature-dependent behavior (contraction of the first interlayer distance and spectacular expansion of the second one), and the effect of anisotropic premelting.

The measurements reported by several authors show that the first interlayer distance in the Al(110) surface is smaller than the respective bulk value by −7%/−11% while the second one is larger by 4.8%/5.5%.[1–5] It has also been observed experimentally that the thermal behavior of the two distances is different.[3,5] For example, the measurements reported in Ref. 5 show that the first interlayer distance exhibits negative thermal expansion, from −8.1% at 100 K to −11.1% at 300 K while the second one shows positive expansion, from 5.5% at 100 K to 6.7% at 300 K (see also Fig. 3). The same tendency, but slightly different values, has been reported in Ref. 3 (see Figs. 7–9).

The anisotropic surface melting below the bulk melting point is observed on the (110) surface of Al and other fcc metals (e.g., Pb and Cu).[7–10] In the case of the Al(110) surface, at about 300 K below the bulk melting point (which is ≈933.5 K at zero pressure), the structure begins to lose a long-range order in the $[1\bar{1}0]$ direction. A few atoms long intact chains begin to migrate along that direction while the periodicity in the [001] direction is still preserved. A quasiliquid layer with residual anisotropy is formed, whose depth and disorder increases with temperature up to the bulk melting point.[10]

Numerous and various theoretical approaches to the above described effects have also been reported, among which the *ab initio* investigations are of particular interest for this work (e.g., Refs. 6 and 11–14). For example, Ref. 14 contains an extended *ab initio* study of low-Miller-index Al surfaces in static-equilibrium condition, i.e., with neither zero-point vibrations nor temperature included. In the work, the effect of computational parameters, such as cutoff energy and *k*-point sampling, as well as the influence of the quantum size effect (QSE) on various physical characteristics of the surfaces have been carefully studied. The work provides a very useful framework for establishing computational conditions when studying particular cases and will be referred to in this paper.

As far as the temperature effects are concerned, two *ab initio* works have been chosen as a reference, to compare and discuss the results obtained in this work. First is an *ab initio* molecular-dynamics simulation, reported in Ref. 6, and the second, Ref. 11, is an extensive study of the surface dynamics in the harmonic regime but gives also simple and convincing arguments explaining the unusual thermal behavior of the Al(110) surface. Both works, although using different methodology, contain a similar observation; there is a strong inverse anisotropy of the mean-square displacements (MSDs) of atoms in the first two layers. First, the MSDs in the [001] direction are significantly larger for the surface atoms than for those in all the other inner layers and second, the MSDs in the direction perpendicular to the surface, [110], are much larger in the second layer than in the first layer, which is connected with the fact that the atoms in the second layer have natural channels of oscillation perpendicular to the surface and directed toward the vacuum. In the work (Ref. 11) a strong coupling between the first and the third layer has been noticed. It is then argued (in both works) that the contraction of the first interlayer distance is due to the displacement of the center of mass of the second layer toward the vacuum (with essentially constant distance between the first and the third layer) because the atoms have a shallower channel in this direction. As a consequence, the contraction of the first interlayer distance is accompanied by the expansion of the second one. In Ref. 6 the nonlinear effects are also reported: the nonlinear increase with temperature of above-mentioned enhanced MSDs.

The investigation into the temperature-dependent structural properties of atomic systems from first principles is a demanding task, generally because it requires scanning either deterministic (MD—molecular-dynamics techniques) or stochastic (MC—Monte Carlo methods) trajectories in multidimensional phase space, which, when one wants to do it *ab initio*, usually involves a huge computational effort. A significant simplification is provided by the harmonic approximation with an underlying assumption that within considered region of phase space the forces acting on ions are linear with respect to displacements. In that case, the computational effort is significantly reduced because the partition function can be evaluated in a quasiclassical way, i.e., the oscillations and their frequencies found either through DFPT (density-functional perturbation theory) or through FD (finite difference) method are quantized, and then the well-known and relatively simple formulas for the partition function can be used. The approach has been widely applied in the so-called quasiharmonic approximation for *ab initio* crystal thermodynamics.[15–20] A major drawback of the harmonic approximation is that it does not take into account the effects involving anharmonic dynamics. However, as it will be discussed in this paper, there is a wide class of systems whose structural behavior can be explained on the ground of the harmonic approximation, including such effects as thermal expansion or even melting. The effects may appear to be the entropy-driven ones, with the harmonic contribution to entropy being crucial.

In this work, a methodology is proposed which is based on that mentioned in Ref. 21 but it has been extended on the idea of the FES in the configurational space spanned by the geometrical, arbitrarily chosen, frozen degrees of freedom. In the first step, the concept of the PES should be recalled. The PES is a key concept in *ab initio* structural investigations within the Born-Oppenheimer approximation. It is just the total energy of a polyatomic system as a function of certain geometrical parameters. The geometrical parameters can be simply the coordinates of all atoms in the system but can also be chosen in a special way, e.g., as the structural parameters of a crystal, as the components of a strain tensor, as planar coordinates of an adsorbate atom on a surface, or quite arbitrarily, basing on the intuition of a researcher. Thus, the PES is a function in certain configurational space, defined by the chosen geometrical parameters. The minima of the function identify the stable or metastable static-equilibrium configurations in that space (at absolute zero temperature and without zeroth quantum vibrations). Moreover, this function determines the system dynamical and thus thermodynamical properties. Therefore PES contains complete information about the structural properties if only the Born-Oppenheimer approximation is valid. The concept of FES is an extension of the PES idea on the case of nonzero temperature. Chosen geometrical parameters are treated as constrained (frozen) and the remaining ones are subjected to the thermodynamical analysis within the concept of the canonical ensemble. The free energy becomes a function in the configurational space of geometrical parameters and contains information about the temperature-dependent structural properties. In particular, the gradients of FES correspond to the generalized stresses (zeros at equilibrium geometries) whereas the second gradients are the generalized elastic constants (all the quantities being now temperature dependent). The zeros of elastic constants at equilibrium geometries indicate the lack of mechanical stability. In principle, the dynamics of a system, necessary for the FES approach, can be analyzed in different ways (e.g., MD, to take into account the anharmonic effects), but in this work, for reasons mentioned in the beginning, the harmonic approximation has been used.

In the study, three effects have been taken into account as potentially giving rise to the observed experimentally phenomena: the bulk-substrate thermal expansion, the effect of asymmetry of PESs, and the entropy-driven shift of the minima of FESs. A brief summary of the theoretical background is given in the following chapters. Then, the technical details and the results of calculations are presented, compared with the results reported in literature, and discussed.

A very satisfactory overall agreement of final results with experimental data has been obtained, although certain discrepancy is observed also in experimental results reported by different authors.[3,5] This work seems to be complementary to previous theoretical works, by offering a different point of view. Thanks to the methodology applied, it has been possible to resolve the relative contribution of different effects to observed phenomena, which leads to better understanding of underlying physics.

II. CONSTRAINED RELAXATION—THE POTENTIAL-ENERGY SURFACE

The quantity on which the well-known concept of PES function is based, is the total energy of a polyatomic system

at fixed ionic positions, $E^{\mathrm{tot}}(\mathbf{R})$, i.e., within the Born-Oppenheimer approximation. The system can be regarded as consisting of two subsystems: the ionic and the electronic one, which can be analyzed separately but not independently. The electronic structure is determined by the positions of ions but at the same time the properties of the ionic system, which are of interest in structural investigations, are determined by the electronic system which forms a kind of "quantum glue" for ions. In the condensed-matter physics, the DFT appears to be the most efficient tool for investigating into the complicated nature of nonuniform electron gas. For the purpose of this work we will confine ourselves to those few general remarks (for review of the field see, e.g., Ref. 22).

We begin the construction by dividing the geometrical parameters of a system into two categories: the ionic coordinates $\mathbf{R}=(R_1,\ldots,R_{N_R})$ and certain geometrical parameters that we will call the constrained ones, denoting them by $\alpha=(\alpha_1,\ldots,\alpha_{N_\alpha})$. The constrained parameters can be, e.g., the volume of a crystal, the structural parameters of a crystal, the components of a strain tensor, but they can also be chosen quite arbitrarily, even as certain atomic coordinates, such as a planar position of an adsorbate atom on a surface. The choice of the constrained parameters depends on the nature of problem and, in a large extent, is a matter of the intuition and experience of a researcher. An illustrating example is presented in this paper.

The total energy becomes a function of atomic coordinates and parameters which describe constraints, $E^{\mathrm{tot}}=E^{\mathrm{tot}}(\mathbf{R},\alpha)$. We define PES as the following function:

$$E^{\mathrm{PES}}(\alpha)=E^{\mathrm{tot}}(\mathbf{R},\alpha)\big|_{\mathbf{R}=\mathbf{R}_{\mathrm{eq}}}, \tag{1}$$

where $\mathbf{R}_{\mathrm{eq}}$ denotes the coordinates of atoms at their equilibrium positions. In other words, PES is the total energy of a system as a function of constrained geometrical parameters with ions relaxed to their equilibrium positions (with respect to the remaining degrees of freedom). If $\alpha\equiv\mathbf{R}$, then $E^{\mathrm{PES}}(\alpha)\equiv E^{\mathrm{tot}}(\mathbf{R})$.

In the structural investigations, besides $E^{\mathrm{PES}}(\alpha)$, the first and the second derivatives of this function are also of great importance. The first derivatives

$$S_i=-\frac{\partial E^{\mathrm{PES}}(\alpha)}{\partial\alpha_i} \tag{2}$$

have the meaning of generalized stresses. For instance, if α_i is an ionic Cartesian coordinate, the S_i is just the ith Cartesian component of force acting on the ion; if α_i is a volume, then S_i has the meaning of pressure; if α_i is a component of the strain tensor, S_i is the corresponding component of the stress tensor, etc.,

The second derivatives

$$K_{ij}=-\frac{\partial S_i}{\partial\alpha_j}=\frac{\partial^2 E^{\mathrm{PES}}(\alpha)}{\partial\alpha_i\,\partial\alpha_j} \tag{3}$$

have the meaning of generalized elastic constants and, in the examples above mentioned, are interpreted respectively as force constants, modulus of compressibility (bulk modulus), components of the elastic tensor, etc. If we deal with an infinite system (such as crystal or crystal surface), a proper normalization is necessary, which has not been included in the formulas above. It should also be noted that the differentiation with respect to α_i involves relaxation of unconstrained ionic coordinates R_{eq}. In some cases (such as, e.g., elastic tensor) the formalism may involve a lot of mathematical complication (see, e.g., Ref. 23) which will not be discussed here.

The $E^{\mathrm{PES}}(\alpha)$ function carries information about basic structural properties of a system, without temperature and quantum zero-point vibration effects. The condition for the extremum of the function is $(S_i=0;\ i=1,\ldots,N_\alpha)$. If it is minimum (either global or local), then it points to the static-equilibrium state (respectively, stable or metastable). For example, this is the condition for equilibrium positions of atoms, equilibrium volume or equilibrium lattice parameters of a crystal. The vanishing second derivative K_{ij} at an extremum $(S_i=0)$ points to the lack of mechanical stability at a given configuration. The behavior of the $E^{\mathrm{PES}}(\alpha)$ function along various directions in the configurational space $\{\alpha\}$ provides information about possible structural transformations.

III. CONSTRAINED DYNAMICS—THE HARMONIC APPROXIMATION

At given constraints, an atomic structure is relaxed and ions are free to move around their equilibrium positions. It is possible then to think about thermodynamics with imposed constraints (constrained thermodynamics). The thermodynamical properties are determined by the dynamical ones, therefore we meet first the problem of constrained dynamics. In computational practice, the problem can be treated by scanning either stochastic or deterministic trajectories using numerous techniques. However, as already mentioned, if one wants to do it from first principles, the task is computationally very demanding. An attractive alternative, employed in this work, is the quasiclassical approach based on the harmonic approximation. The main drawback of this approach is that it neglects the anharmonic contribution to entropy. However, as it will be shown, the harmonic contribution to entropy can be crucial in the entropy-driven effects. There is also a simple way to account for nonlinearity connected with the deviation of constraints, as will be demonstrated in this paper.

According to the definition of $E^{\mathrm{PES}}(\alpha)$, at a fixed value of the α vector all the unconstrained atomic degrees of freedom $(\mathbf{R})$ are relaxed to their equilibrium values $(\mathbf{R}_{\mathrm{eq}})$. The function $E^{\mathrm{tot}}(\alpha,\mathbf{R})$ plays the role of potential energy for ions and can be approximated by the second-order power series with respect to ionic displacements from equilibrium positions. The forces on ions become then linear with respect to the displacements and dynamics is harmonic (the smaller are the displacements, the better is the approximation). The eigenfrequencies and corresponding polarization vectors $\{\omega_n,\mathbf{A}_n\}$, the independent harmonic modes of oscillation (normal modes), are found from the eigenvalue problem

$$\hat{\Phi}\mathbf{A}=\omega^2\mathbf{A}, \tag{4}$$

where

$$\hat{\Phi} = [\Phi_{ij}(\alpha)] = \left[\frac{1}{\sqrt{M_i M_j}} \frac{\partial^2 E^{\text{tot}}(\alpha, \mathbf{R})}{\partial R_i \, \partial R_j} \right]_{R=R_{\text{eq}}} \tag{5}$$

is the force-constant matrix of the system, i,j label the unconstrained ionic coordinates, and M_i is the ionic mass associated with ith unconstrained coordinate. One should note that the force constants and therefore the eigenfrequencies and polarization vectors are now α-vector dependent.

As a result we get a discrete spectrum of normal modes whose number is equal to the number of unconstrained ionic degrees of freedom. In the case of infinite periodic systems, the translational symmetry is used to reduce the force-constant matrix to the dynamical matrix which becomes the wave-vector dependent and the normal modes are additionally classified by a wave vector k belonging to the first Brillouin zone (BZ). Any state of system vibration is a linear superposition of normal modes. Thus, from the point of view of thermodynamics, the real system is equivalent to the system of independent (or weakly interacting) harmonic oscillators whose thermodynamical analysis is straightforward.

The *ab initio* calculation of the force-constant matrix is a separate problem and will not be discussed here in detail. The second derivatives in Eq. (5) can be calculated either from the DFPT (Refs. 24–27) or from the FD (Refs. 28 and 29) method with the use of the Hellmann-Feynman forces.

IV. CONSTRAINED THERMODYNAMICS—THE FREE-ENERGY SURFACE

The thermodynamical analysis is performed within the concept of canonical ensemble (system is in contact with the thermostat of temperature T). The Helmholtz free energy is the proper thermodynamical function to be considered in the case of geometrical constraints since it is minimized at equilibrium in such conditions (e.g., constant volume and temperature for a crystal).

The statistical thermodynamics gives the general formula for the free energy,

$$F = -\frac{\ln(Z)}{\beta}, \tag{6}$$

where $Z=\Sigma_i \exp(-\beta E_i)$ is the partition function, $\beta=1/(k_B T)$, k_B is the Boltzmann constant, and the summation runs over all the microstates.

The formula above leads to the concept of FES which is simply the free energy as a function of geometrical parameters describing constraints. The energy of the system contains two parts: the static one, equal to the value of $E^{\text{PES}}(\alpha)$ function at the fixed configuration α, and the dynamical part $E^d(\alpha)$, connected with the dynamics of atoms along unconstrained coordinates,

$$E = E^{\text{PES}}(\alpha) + E^d(\alpha). \tag{7}$$

The partition function then takes the form

$$Z = \sum_i \exp[-\beta(E^{\text{PES}} + E_i^d)] = \exp(-\beta E^{\text{PES}}) Z^d, \tag{8}$$

where $Z^d=\Sigma_i \exp(-\beta E_i^d)$ is the dynamical part of the partition function and the summation runs over the microstates corresponding to this dynamics. Thus, the free energy, apart from being a function of temperature, is also a function of the constrained degrees of freedom α and becomes the FES,

$$F^{\text{FES}}(T,\alpha) = E^{\text{PES}}(\alpha) - \frac{1}{\beta}\ln[Z^d(T,\alpha)]. \tag{9}$$

It can be seen above that F^{FES} differs from E^{PES} by the temperature-dependent dynamical part. As in the case of $E^{\text{PES}}(\alpha)$, the first and the second derivatives of $F^{\text{FES}}(\alpha)$ are very informative,

$$S_i(T,\alpha) = -\frac{\partial F^{\text{FES}}(T,\alpha)}{\partial \alpha_i} \tag{10}$$

and

$$K_{ij}(T,\alpha) = \frac{\partial^2 F^{\text{FES}}(T,\alpha)}{\partial \alpha_i \, \partial \alpha_j} \tag{11}$$

having the same interpretation as in the case of E^{PES}; the generalized stresses and the generalized elastic constants (isothermal), which are both temperature-dependent now.

The quasiclassical approach together with the harmonic approximation allow to calculate easily the thermodynamic functions. The normal modes (independent oscillators) are quantized and the summation over the microstates in Eq. (6) denotes the summation over quantum states. The dynamical part of the partition function [Eq. (8)] takes the form

$$Z^d = \prod_i Z_i, \tag{12}$$

where Z_i is the single-quantum oscillator partition function given by

$$Z_i = \frac{\exp[-\beta\hbar\omega_i(\alpha)/2]}{1-\exp[-\beta\hbar\omega_i(\alpha)]}. \tag{13}$$

The free energy is the sum of the single-oscillator free energies and the static part (both α dependent),

$$F^{\text{FES}}(\alpha) = E^{\text{PES}}(\alpha) + \sum_i F_i(\alpha). \tag{14}$$

One can evaluate now the first derivative [Eq. (10)] of $F^{\text{FES}}(\alpha)$ within the harmonic approximation

$$\Phi_k(T,\alpha) = -\frac{\partial F^{\text{FES}}(T,\alpha)}{\partial \alpha_k} = S_k(\alpha) + \frac{1}{\alpha_k}\sum_i U_i(\alpha)\gamma_i^k(\alpha), \tag{15}$$

where $S_k(\alpha)$ is the static contribution, Eq. (2),

$$U_i(\alpha) = \frac{\hbar\omega_i(\alpha)}{2}\frac{\{1+\exp[-\beta\hbar\omega_i(\alpha)]\}}{\{1-\exp[-\beta\hbar\omega_i(\alpha)]\}} \tag{16}$$

is the contribution of the ith normal mode to the internal energy and

$$\gamma_i^k(\alpha) = -\frac{\partial \ln[\omega_i(\alpha)]}{\partial \ln[\alpha_k]} \tag{17}$$

is the Grüneisen number. As it can be seen in Eq. (10), the evaluation of generalized stresses at a given α vector within

harmonic approximation requires the calculation of normal-mode frequencies as well as their first derivatives with respect to α. The second derivatives (generalized elastic constants) can be found either by the FD method or by analytical differentiation of Eq. (14) which would lead, however, to mixed second derivatives of $\omega_i(\alpha)$.

V. EXAMPLE: THE fcc Al CRYSTAL

The quasiharmonic approximation is a well-known idea. So far, many papers dealing with *ab initio* crystal thermodynamics based on that approach have been published, e.g., Refs. 15–20. The crystal thermodynamics is treated within the harmonic approximation with the assumption that the phonon frequencies depend on crystal volume. Using the language presented in this work, it becomes just a particular case of applying the FES concept. For the purpose of this work, the aluminum thermal-expansion curve calculated from first principles is needed. For this reason, and also to show the consistency of the quasiharmonic approximation with the FES language, chosen results published in Ref. 19 are presented below.

Let the crystal volume be considered as the constrained degree of freedom: $\alpha=V$. The partition function and the free energy Eqs. (13) and (14) now read

$$Z_i = \frac{\exp[-\beta\hbar\omega_i(V)/2]}{1-\exp[-\beta\hbar\omega_i(V)]}, \tag{18}$$

$$F^{\mathrm{FES}}(V) = \sum_i F_i(V) + E^{\mathrm{PES}}(V), \tag{19}$$

where the summation consists of the integration over the Brillouin zone and the summation over phonon branches. The free energy is a function of volume and it becomes FES.

The first derivative has the meaning of pressure

$$P(T,V) = -\frac{\partial F^{\mathrm{FES}}(T,V)}{\partial V}. \tag{20}$$

This is an equation of state which in that approach takes the form called the Mie-Grüneisen equation of state,

$$P(V,T) = P_0(V) + \frac{1}{V}\sum_i U_i\gamma_i, \tag{21}$$

where P_0 is the static contribution to pressure, equal to $-\partial E^{\mathrm{PES}}(V)/\partial V$, U_i is the single-mode contribution to the internal energy, Eq. (16), and $\gamma_i=-d[\ln(\omega_i)]/d[\ln(V)]$ is the volume-dependent Grüneisen number. The Grüneisen number is normal-mode specific, therefore must be indexed by i.

The second derivative normalized to the unit volume is the bulk modulus (isothermal modulus of elasticity) and gets the analytical form

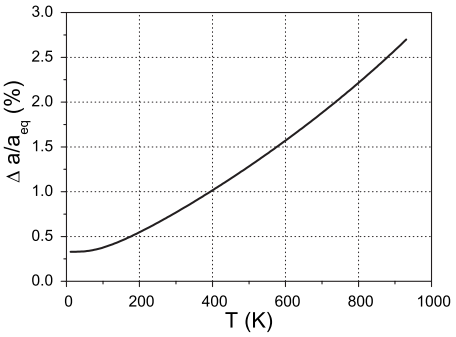

FIG. 1. The relative variation in the fcc Al lattice constant as a function of temperature, calculated *ab initio* (LDA) (the static-equilibrium value of the lattice constant is 3.974 Å) (Ref. 19).

$$B(T,V) = V\frac{\partial^2 F^{\mathrm{FES}}(T,V)}{\partial V^2} = B_{T0} + (P-P_0) + \frac{1}{V}\sum_i \gamma_i^2(U_i - C_iT) - \sum_i U_i\frac{\partial\gamma_i}{\partial V}, \tag{22}$$

where B_{T0} is the static contribution and

$$C_i = \frac{k_B\beta^2\hbar\omega_i^2\exp(-\beta\hbar\omega_i)}{[1-\exp(-\beta\hbar\omega_i)]^2} \tag{23}$$

is the single-mode contribution to the constant volume specific heat.

In the equation of state [Eq. (21)], any pair of variables, among temperature, volume, and pressure, can be taken as independent, and next, via the Maxwell's thermodynamic relations, all the thermodynamic functions can be evaluated. For the purpose of this work, however, we are interested only in the volume thermal expansion [temperature-dependent shift of the $F^{\mathrm{FES}}(V,T)$ minimum].

The fcc Al thermal-expansion curve, Fig. 1,[19] has been calculated *ab initio*, within local density approximation (LDA) (Ceperley-Alder/Perdew-Zunger[30,31]). The Al pseudopotential has been generated with the use of FHI98PP code,[32] with the nonlocal core-valence exchange-correlation interaction included. All the calculations for crystal (the ground state and the linear-response function) have been done with the use of the ABINIT (Ref. 33) code. The cutoff energy of $E_{\mathrm{cut}}=20$ Hartree and $(6\times6\times6)$ Monkhorst-Pack k-points mesh,[34] shifted by (0.5,0.5,0.5), (0.5,0.0,0.0), (0.0,0.5,0.0), and (0.0,0.0,0.5), have been applied. The same set of special k points was used in the calculation of the electronic ground state, the response function, and in the calculation of the phonon partition function. The choice of all the parameters has been preceded by a careful study of convergence. The Murnaghan equation of state[35] has been used to fit the static contribution to the free energy, $E^{\mathrm{PES}}(V)$. The second-order polynomial has been used to fit the $\omega_i(V)$. It should be added that the curve in Fig. 1 corresponds to the calculated *ab initio* thermal-expansion coefficient [Fig. 4a in Ref. 19] whose agreement with experimental data is very good.

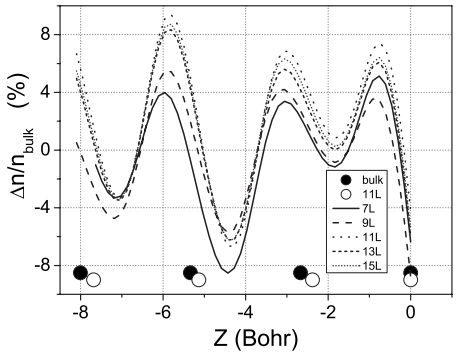

FIG. 2. The relative change (with respect to the bulk reference value) in the electronic density averaged over the surface cell, as a function of distance from the surface (Fridel oscillations), and for different number of atomic layers in the slab (7,9,11,13,15); open circles show bulk positions of Al ions and black circles—their relaxed surface positions calculated for a 11-layer slab. The convergence can be observed pointing to the 11-layer slab as the minimum one giving converged result.

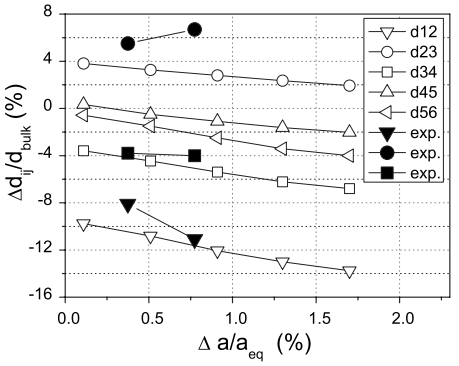

FIG. 3. The relaxation of atomic layers in the 11-layer symmetrical slab, represented in terms of interlayer distances (d_{ij}), as a function of deviation of the bulk lattice constant from its equilibrium value. The positions of black dots represent experimental values (Ref. 5) corresponding to $T=100$ K and $T=300$ K (respective lattice deviations according to Fig. 1).

VI. Al(110) SURFACE

The methodology above presented has been applied to investigate the temperature-dependent structural properties of the Al(110) surface. First, we consider the temperature-dependent multilayer relaxation and its intriguing behavior described in the introduction. Three mechanisms have been identified as contributing to the phenomenon: (i) the effect of thermal expansion of the bulk substrate, (ii) the shift of average interlayer distances due to asymmetry of E^{PES}, and (iii) the entropy-driven shift of interlayer distances. To start the investigation, it was necessary to establish the model for *ab initio* calculations. A standard approach of repeated slab geometry has been applied. The additional technical parameters (to those appearing in the bulk calculations)—the number of atomic layers in the slab and vacuum thickness—have been subjected to thorough convergence tests. Particularly, the slab thickness is a critical parameter for two reasons: the well-known QSE (see Refs. 13 and 14) and the necessity to avoid interaction between two surfaces. The vacuum thickness must be big enough to avoid the interaction between adjacent slabs. Since the problem appeared to be computationally very demanding, the model parameters had to be chosen very carefully, as a result of a compromise between required accuracy and reasonable needs for computational resources. As a result of many tests, such as convergence of electronic density near the surface (Fig. 2) or convergence of static multilayer relaxation, with respect to the number of atomic layers (from 7 up to 15), it has been found that the 11-layer symmetric slab is the minimum one guaranteeing acceptable accuracy on the one hand and reasonable requirements for computational resources on the other (see also Refs. 13 and 14). The vacuum thickness of 11 Å has been found to be sufficient to avoid interaction between adjacent slabs. To make the calculations consistent with these previously done for the bulk,[19] the same parametrization of XC functional (LDA, Ceperley-Alder/Perdew-Zunger[30,31]) and the same pseudopotential have been used, the cutoff energy has been set to $E_{\mathrm{cut}}=20$ Hartree and $(8\times12\times1)$ Monkhorst-Pack k-points mesh, shifted by (0.5,0.5,0.5) has been applied. The surface lattice constant has been set to the bulk static-equilibrium value [3.974 Å (Ref. 19)]. All the calculations for slabs reported in this paper have been done with the use of the ABINIT code.[33]

Below, the results of calculations for the three above-mentioned mechanisms and the final results are presented and discussed.

A. Effect of bulk-substrate thermal expansion

The bulk crystal lattice thermal expansion is the effect independent of the surface properties but appears to have a significant influence on those properties. A crystal surface can be thought of as an atomic system placed on the bulk substrate. The location of the bulk-surface border can be roughly estimated from the local properties, i.e., at certain depth they should not differ from those of the bulk. Since the crystal lattice constant varies with temperature, the bulk substrate acts as a rigid "piston" stretching or compressing the surface. In this work, the influence of the bulk-substrate thermal expansion on the interlayer distances has been studied. The effect is shown in Fig. 3 and in Figs. 7–9 (thin solid line). The expansion of the bulk lattice (represented in the graphs either as the relative variation in the lattice constant or temperature) results in contraction of all the interlayer distances. In the same figure, respective experimental values are shown (according to Ref. 5). The relationship between the value of the bulk constant and temperature has been found from the previously *ab initio* calculated Al crystal thermal-expansion curve (Fig. 1).

B. Effect of asymmetry of potentials

To study PESs and FESs, it is necessary to choose some constraints. Examples of constraints are shown in Fig. 4. However, these are not the only possibilities, one can choose, e.g., a constraint coupling the first and the third layer d_{13} (to study the effect of the coupling, important as stated in Ref.

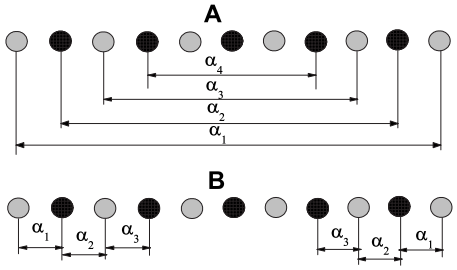

FIG. 4. Examples of the choice of constraints in the 11-layer symmetrical slab for an investigation into the temperature-dependent multilayer relaxation. Other configurations are also possible (e.g., a constraint coupling the first and the third layer, d_{13}, etc.). In this work, the configuration B has been exploited, in which the constraints refer directly to interlayer distances: $\alpha 1 = d_{12}$, $\alpha 2 = d_{23}$, and $\alpha 3 = d_{34}$.

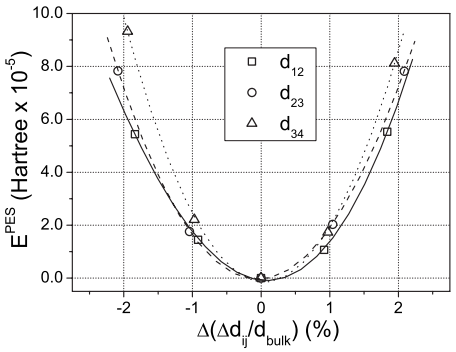

FIG. 5. PESs for the constraints α chosen as interlayer distances (the case B in Fig. 4). On the horizontal axis, there is a deviation from equilibrium distance expressed in percentage of reference bulk distance. The equilibrium distances are $d_{12} = -8.08\%$, $d_{23} = 4.28\%$, and $d_{34} = -2.81\%$.

11) or any other configuration that would provide a significant information about the system. The author of this work tested both configurations shown in Fig. 4, although in this paper only the results corresponding to configurations "B" (α parameters directly referring to interlayer distances d_{ij}) are reported. In principle, the α parameters span three-dimensional (3D) configurational space but the evaluation of FES in 3D space involves enormous complication such as scanning phonon frequencies in 3D space, minimization in 3D, etc. The advantage of such an approach would be a direct inclusion of coupling between constraints but the disadvantage is less degree of freedom contributing to entropy and therefore the entropy-driven effects poorly reproduced. Here, a simplified approach has been applied, namely, the constraints have been applied independently, one by one, i.e., at every constraint the FES was a function of only one variable.

The parameters $\alpha 1 = d_{12}$, $\alpha 2 = d_{23}$, and $\alpha 3 = d_{34}$ have been varied between -2% and $+2\%$ of the reference bulk distance with respect to their equilibrium values which have been found to be $d_{12} = -8.08\%$, $d_{23} = 4.28\%$, and $d_{34} = -2.81\%$ (the values agree well with the results reported by Da Silva[14] for an 11-layer slab: $-8.18\%, +3.93\%, -2.87\%$, respectively; the differences, especially for d_{23}, can be attributed to a more exact method—full-potential linearized plane wave—used there). Thus, at five points in that range the whole structure was relaxed (except for the constrained degrees of freedom), the *ab initio* total energies were calculated and the third-order polynomial fitted to the results. A convenient feature of the ABINIT code—the possibility to perform the constrained relaxation—has been exploited. The resulting PESs are shown in Fig. 5. The fitted curves have been used to find the thermodynamical average of every α parameter as a function of temperature. In the regime of dynamics confined to the adiabatic variation in constraints, the thermodynamical average can be found from the formula

$$\bar{\alpha}(T) = \frac{\int \alpha \exp[-E^{\mathrm{PES}}(\alpha)/(k_B T)] d\alpha}{\int \exp[-E^{\mathrm{PES}}(\alpha)/(k_B T)] d\alpha}. \tag{24}$$

The results are shown in Figs. 7–9 (thin dash line). A slight asymmetry of potential-energy surfaces results in the temperature-dependent shift of interlayer distances. The effect, however, appears to be inconspicuous in comparison with the other two.

C. Entropy-driven shift

The entropy-driven shift is connected with the displacement of the minimum of FES. It is named the "entropy-driven" because it is mainly the entropy contribution to free energy which is responsible for the displacement: the system "moves" toward lower frequencies to increase entropy, even if the internal energy increases. To find the free energy from the formula (9), it was necessary to study the dynamics of the system. This was done within the harmonic approximation as described in Sec. III. Since finding the full phonon band structure appeared to be an extremely demanding computational task (according to the author's experience it was about three months of CPU time per one series of calculations), for the purpose of this work only the Γ-point vibrations have been used. At such approximation the problem reduces formally to the dynamics of the 11-atom chain. From 33 degrees of freedom, four are frozen (because of constraints). The diagonalization of the 29×29 dynamical matrix gives 29 eigenfrequencies among which two have zero value (correspond to the acoustic modes) and must be excluded from the partition function.

The calculations of the dynamical matrix have been done with the use of the finite difference (FD) method. For all the constraints: $\alpha 1$, $\alpha 2$, and $\alpha 3$ (configuration B in Fig. 4) and at four points around their equilibrium values, the structure was relaxed, phonon spectra found, and the second-order polynomial fitted to the data. An example of the phonon energy as a function of the value of constraint $\alpha 2$, is presented in Fig. 11. In the next step, the free energies as functions of α values have been evaluated from the formula (14). An example of, obtained in that way, FESs, for the constraint $\alpha 2 (d_{23})$ and five temperatures is presented in Fig. 6. The shift of the $F^{\mathrm{FES}}(\alpha)$ minimum can be clearly seen. Its temperature-dependent position has been found from the root of the function (15) and it represents the entropy-driven shift of the interlayer distance. The shifts corresponding to the first three

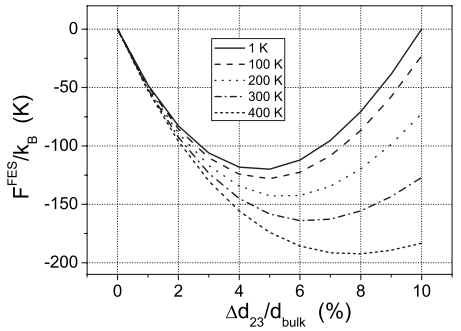

FIG. 6. The free-energy surfaces (F^{FES}) for $\alpha=d_{23}(\alpha 2)$, for five temperatures. A distinct shift of the minimum can be observed.

interlayer distances are shown in Figs. 7–9 (dash-dot line).

It should be mentioned that the calculation of the free-energy surface appeared to be a difficult computational task. Since the partition function and the free energy are very sensitive to phonon frequency values, their evaluation must have been done with very high accuracy. For example, in the calculations presented here the forces acting on atoms have been converged down to 10^{-8} Hartree/Bohr, at maximum forces having values on the order of 10^{-3} Hartree/Bohr. Many trials had been done before acceptable stability of results was achieved. About ten days of CPU time on a typical high-power computer was needed for one series of calculations. Here, the representative results are shown.

D. Final results

The temperature-dependent values of interlayer distances d_{12}, d_{23}, and d_{34} have been taken as a superposition of three above discussed effects and they are shown in Figs. 7–9 (thick solid line), together with all three contributions. The following conclusions can be drawn from the figures: (i) the thermal contraction of the first interlayer distance, d_{12}, is mainly due to the thermal expansion of the bulk substrate;

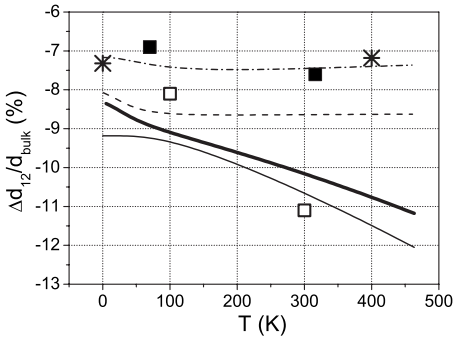

FIG. 7. Temperature-dependent variation in d_{12} interlayer distance (thick solid line) as a superposition of three effects: bulk-substrate thermal expansion (thin solid line), asymmetry of E^{PES} (dash line), entropy-driven shift (dash-dot line); experimental results according to Ref. 5 (empty squares) and Ref. 3 (solid squares), results of *ab initio* MD (Ref. 6) (stars). In this case, the bulk thermal expansion plays a crucial role and leads to significant contraction of the interlayer distance (the contraction rate is about two times higher than the bulk thermal-expansion rate).

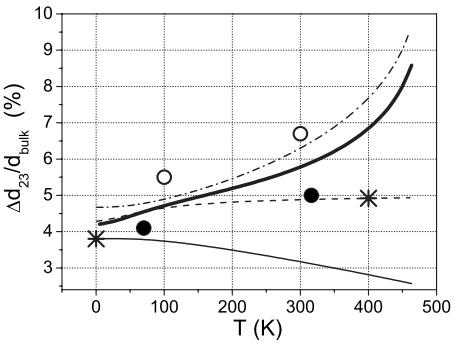

FIG. 8. Temperature-dependent variation in d_{23} interlayer distance (thick solid line) as a superposition of three effects: bulk-substrate thermal expansion (thin solid line), asymmetry of E^{PES} (dash line), entropy-driven shift (dash-dot line); experimental results according to Ref. 5 (empty circles) and Ref. 3 (solid circles), results of *ab initio* MD (Ref. 6) (stars). In this case, the entropy-driven shift plays a crucial role and leads to spectacular expansion.

the effect of asymmetry and the entropy-driven shift do not play here an important role (both are relatively small), (ii) the spectacular thermal expansion of the second interlayer distance, d_{23}, is caused by the entropy-driven shift which predominates over the other two effects; the distinct softening mode, seen in Fig. 11 (thick solid line), has been identified as responsible for the spectacular expansion (the mode was just removed from the partition function and the expansion disappeared); such a softening mode has not been observed at the other two constraints, (iii) the three contributions nearly cancel to zero in the case of the third interlayer distance, d_{34}, which remains almost constant with changing temperature. The overall agreement with the experimental values is very satisfactory.

In Figs. 7–9 also the results of *ab initio* molecular-dynamics simulation[6] are presented, together with experimental results.[3] In the reported MD simulation all the three effects considered here are included. The authors take into account the bulk thermal expansion (the empirical thermal-

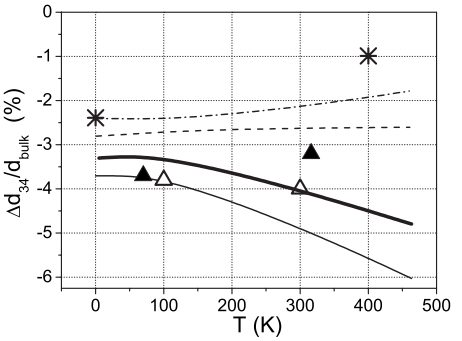

FIG. 9. Temperature-dependent variation in d_{34} interlayer distance (thick solid line) as a superposition of three effects: bulk-substrate thermal expansion (thin solid line), asymmetry of E^{PES} (dash line), entropy-driven shift (dash-dot line); experimental results according to Ref. 5 (empty triangles) and Ref. 3 (solid triangles), results of *ab initio* MD (Ref. 6) (stars). In this case, the three effects almost cancel each other, which leads to nearly no variation in the distance with temperature.

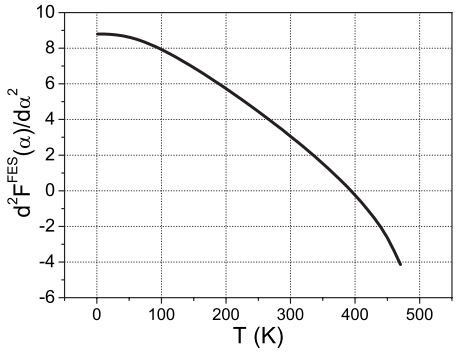

FIG. 10. The second derivative $\frac{\partial^2 F^{\mathrm{FES}}(\alpha)}{\delta \alpha^2}$, for $\alpha = d_{23}$, as a function of temperature. The zero of the function (at ≈400 K) points to the loss of stability.

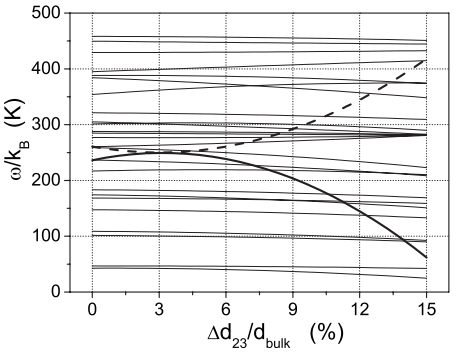

FIG. 11. The dependence of phonon frequencies on the d_{23} interlayer distance. Two characteristic modes can be observed: the rapidly softening one (thick solid line) and rapidly hardening one (thick dash line). The softening mode is responsible for the entropy-driven increase in d_{23} interlayer distance and for the loss of stability of the structure at ≈400 K. The polarization of the softening mode (see Sec. VI E) points to its connection with the anisotropic surface melting. The hardening mode is mainly a relative oscillation of the first two atomic layers in the vertical to the surface direction and points to partial detachment of the two layers from the rest of the crystal.

expansion coefficient is applied to *ab initio* equilibrium lattice constant). However, in MD simulation it is rather difficult to distinguish between the nonlinear effects and the entropy-driven ones, although both can be present. It is also difficult to tell what is the effect of the bulk thermal expansion. In other words, the relative contributions of different effects are somewhat hidden in the MD simulation, although, the overall agreement with experimental data is very good. The approach presented in this work allows to resolve the relative contribution, at least partially. For example, it has been found in this work that the contraction of the first interlayer distance is mainly due to the bulk thermal expansion, which seems to contradict the conclusion in Ref. 6 (which attributes the contraction rather to the shallower potential channel for atoms from the second layer toward the vacuum). However, the effect of the bulk thermal expansion was present in the MD simulation, only its contribution may be could not be noticed.

E. Reference to anisotropic surface melting

An interesting reference to the observed experimentally anisotropic surface melting (see Sec. I) can be found in the results obtained in this work. Figure 10 shows the temperature dependence of the second derivative of $F^{\mathrm{FES}}(\alpha 2)$ calculated at its minimum. At ≈400 K the function crosses the zero line, which according to the theory (Sec. IV) is an indication of the loss of stability. In other words, starting from certain temperature (≈400 K in this case) the function $F^{\mathrm{FES}}(\alpha)$ (Fig. 6) does not have a distinct minimum any more. Moreover, it has been checked that the softening mode seen in Fig. 11 (thick solid line) is responsible for the loss of stability. Its polarization has been also found and will be represented here in the basis whose unit vectors are oriented as follows: $[([001],[1\bar{1}0],[110]),\ldots]$, for each atom in the 11-atom chain in a supercell. Thus, the polarization of the softening mode in the initial part of the $\omega(\alpha)$ curve is as follows: $[(0,-0.28,0),(0,0.31,X),(0,0.25,X),(0,-0.42,0),(0,-0.06,0),(0,0.41,0),\ldots]$, where *Xs* stand here for the frozen degrees of freedom and the three dots at the end denote the second, symmetric part of the polarization vector (the rest of the atoms). Clearly the displacements of all the atoms in the softening mode are in the $[1\bar{1}0]$ direction, exactly along which the loss of the long-range order has been observed experimentally. The loss of stability appears at ≈400 K, which is much lower than the bulk melting point, and this also agrees (at least qualitatively) with the experimental observation. Moreover, one can conclude, when looking at the polarization vector, that the second and the third layer perform a synchronous oscillation with opposite phase to oscillating synchronously the first and the fourth layer. However, it is difficult to draw any conclusion from that fact at this stage since it is not sure what is the effect of the finite size of the system on the oscillations and how the polarization evolves with increasing α.

It should be mentioned that the premelting on Al(110) surface is a complicated process and still seems to be a controversial issue. As the experiment shows,[36] with increasing temperature the premelting is preceded by the proliferation of point defects and surface roughness. This fact has been also confirmed by theoretical works.[6,37] The controversy concerns the residual anisotropy: in the experiment reported in Ref. 36, the residual short-range order was observed in both directions, $[1\bar{1}0]$ and $[001]$, and the quasiliquid layer supposed to be formed by migrating clusters rather than intact atomic chains. In turn, the MD simulation[6] shows an enhanced MSD in the direction $[001]$, which might rather be expected along $[1\bar{1}0]$. The present work provides one more piece of information: there exists a distinct anisotropic loss of stability in the direction $[1\bar{1}0]$. This agrees also with the conclusions of MD simulation reported in Ref. 36 where the residual order was observed preferentially in that direction. The fact that the MSD is smaller along $[1\bar{1}0]$ can be due to a relatively small contribution of the softening modes (the one in the center of BZ, identified in this work and probably also

adjoining modes) to the MSD (one should note that the loss of stability can be caused even by a single mode).

The softening of the above described mode is accompanied by the hardening of another mode (thick dash line in Fig. 11). Its polarization has been found to be $[(0,0,-0.7),(0,0,X),(0,0,X),(0,0,0.003),(0,0,-0.001),(0,0,0),\ldots]$.

This mode appears to be mainly a relative oscillation of the first layer with respect to the second one. The hardening of this mode can be explained in the following way: the thermal expansion of the second interlayer distance causes partial "detachment" of the first two layers from the rest of the crystal (weakening of bonding between first two layers and the rest of the crystal) and therefore the strengthening of bonding between the two layers, which in turn results in an increase in the frequency of relative oscillation.

The conclusions above drawn correspond nicely with the observation that in the second interlayer region a significant decrease in electronic density appears, $\approx 10\%$ of the bulk value (Fig. 2).

VII. CONCLUSIONS

A number of approximations have been used in this work. First, the local density approximation for the exchange-correlation energy and the norm-conserving pseudopotential, which are both typical of the calculations based on the density-functional theory. Second, the harmonic approximation for lattice dynamics with only Γ-point vibrations taken into account, and second-order polynomial approximation for the $\omega(\alpha)$ dependence. Third, treating the constraints independently, one by one. Finally, treating the three considered physical effects as independent (in principle, they are not). In spite of that, very satisfactory results have been obtained and two main goals have been achieved. The first one is the better understanding of physical effects staying behind the temperature-dependent structural behavior of the Al(110) surface and the second is the demonstration that the methodology based on the concepts of PES and FES joined with the harmonic approximation is an effective scientific tool in the analysis of temperature-dependent structural properties of a certain class of systems. Whether the methodology can be applied to a particular case is always an open question, but the successful, in the author's opinion, attempt presented here opens promising perspectives.

It should be pointed out that the analysis in this work has been performed in the harmonic regime, except for the nonlinearity of forces associated with the variation in constraints. This is certainly the disadvantage of the approach, but, in principle, the presented methodology allows to include the anharmonic dynamics (e.g., MD simulation at imposed geometrical constraints). However, as the results show, the harmonic contribution to the free energy may appear to be crucial in explaining such effects as the thermal expansion and even premelting, if they are the entropy driven.

ACKNOWLEDGMENTS

Special acknowledgments are due to Jörg Neugebauer for his inspiration. The author also would like to thank Jerzy Peisert for his assistance. All the calculations for this work have been done in Wroclaw Center for Networking and Supercomputing.

*pawel.scharoch@pwr.wroc.pl

[1] J. N. Andersen, H. B. Nielsen, L. Petersen, and D. L. Adams, J. Phys. C: Solid State Phys. **17**, 173 (1984).
[2] J. Noonan and H. L. Davis, Phys. Rev. B **29**, 4349 (1984).
[3] H. Gobel and P. von Blanckenhagen, Phys. Rev. B **47**, 2378 (1993).
[4] B. W. Busch and T. Gustafsson, Surf. Sci. **415**, L1074 (1998).
[5] A. Mikkelsen, J. Jiruse, and D. L. Adams, Phys. Rev. B **60**, 7796 (1999).
[6] N. Marzari, D. Vanderbilt, A. De Vita, and M. C. Payne, Phys. Rev. Lett. **82**, 3296 (1999).
[7] J. W. M. Frenken, B. J. Hinch, J. P. Toennies, and Ch. Wöll, Phys. Rev. B **41**, 938 (1990).
[8] A. W. Denier van der Gon, H. M. van Pinxteren, J. W. M. Frenken, and J. F. van der Veen, Surf. Sci. **244**, 259 (1991).
[9] W. Theis and K. Horn, Phys. Rev. B **51**, 7157 (1995).
[10] M. Pŏlcik, L. Wilde, and J. Haase, Phys. Rev. Lett. **78**, 491 (1997).
[11] S. Narasimhan, Phys. Rev. B **64**, 125409 (2001).
[12] K. M. Ho and K. P. Bohnen, Phys. Rev. B **32**, 3446 (1985).
[13] A. Kiejna, J. Peisert, and P. Scharoch, Surf. Sci. **432**, 54 (1999).
[14] J. L. F. Da Silva, Phys. Rev. B **71**, 195416 (2005).
[15] A. Debernardi, M. Alouani, and H. Dreysse, Phys. Rev. B **63**, 064305 (2001).
[16] J. Xie, S. de Gironcoli, S. Baroni, and M. Scheffler, Phys. Rev. B **59**, 965 (1999).
[17] A. A. Quong and A. Y. Liu, Phys. Rev. B **56**, 7767 (1997).
[18] S. Biernacki and M. Scheffler, Phys. Rev. Lett. **63**, 290 (1989).
[19] P. Scharoch, J. Peisert, and K. Tatarczyk, Acta Phys. Pol. A **112**, 513 (2007).
[20] F. Körmann, A. Dick, B. Grabowski, B. Hallstedt, T. Hickel, and J. Neugebauer, Phys. Rev. B **78**, 033102 (2008).
[21] J. Xie, S. de Gironcoli, S. Baroni, and M. Scheffler, Phys. Rev. B **59**, 970 (1999).
[22] R. M. Martin, *Electronic Structure, Basic Theory and Practical Methods* (Cambridge University Press, Cambridge, England, 2003).
[23] X. Wu, D. Vanderbilt, and D. R. Hamann, Phys. Rev. B **72**, 035105 (2005).
[24] S. Baroni, S. de Gironcoli, and A. D. Corso, Rev. Mod. Phys. **73**, 515 (2001).
[25] S. de Gironcoli, Phys. Rev. B **51**, 6773 (1995).
[26] X. Gonze, Phys. Rev. B **55**, 10337 (1997).
[27] X. Gonze and C. Lee, Phys. Rev. B **55**, 10355 (1997).
[28] K. Parlinski and Y. Kawazoe, Phys. Rev. B **60**, 15511 (1999).
[29] P. Scharoch, K. Parlinski, and A. Kiejna, Acta Phys. Pol. A **97**, 349 (2000).
[30] D. M. Ceperley and B. J. Alder, Phys. Rev. Lett. **45**, 566 (1980).

[31] J. P. Perdew and A. Zunger, Phys. Rev. B **23**, 5048 (1981).
[32] M. Fuchs and M. Scheffler, Comput. Phys. Commun. **119**, 67 (1999).
[33] X. Gonze, J.-M. Beuken, R. Caracas, F. Detraux, M. Fuchs, G.-M. Rignanese, L. Sindic, M. Verstraete, G. Zerah, F. Jollet, M. Torrent, A. Roy, M. Mikami, Ph. Ghosez, J. -Y. Raty, and D. C. Allan, Comput. Mater. Sci. **25**, 478 (2002).
[34] H. Monkhorst and J. Pack, Phys. Rev. B **13**, 5188 (1976).
[35] F. Murnaghan, Proc. Natl. Acad. Sci. U.S.A. **30**, 244 (1944).
[36] L. Pedemonte, G. Bracco, A. Robin, and W. Heiland, Phys. Rev. B **65**, 245406 (2002).
[37] D. Shu, D. Sun, X. Gong, and W. Lau, Surf. Sci. **441**, 206 (1999).